

# An efficient algorithm based on splitting for the time integration of the Schrödinger equation

Sergio Blanes<sup>1\*</sup>    Fernando Casas<sup>2†</sup>    Ander Murua<sup>3‡</sup>

April 13, 2018

## Abstract

We present a practical algorithm based on symplectic splitting methods to integrate numerically in time the Schrödinger equation. When discretized in space, the Schrödinger equation can be recast as a classical Hamiltonian system corresponding to a generalized high-dimensional separable harmonic oscillator. The particular structure of this system combined with previously obtained stability and error analyses allows us to construct a set of highly efficient symplectic integrators with sharp error bounds and optimized for different tolerances and time integration intervals. They can be considered, in this setting, as polynomial approximations to the matrix exponential in a similar way as methods based on Chebyshev and Taylor polynomials. The theoretical analysis, supported by numerical experiments, indicates that the new methods are more efficient than schemes based on Chebyshev polynomials for all tolerances and time intervals. The algorithm we present incorporates the new splitting methods and automatically selects the most efficient scheme given a tolerance, a time integration interval and an estimate on the spectral radius of the Hamiltonian.

<sup>1</sup>Instituto de Matemática Multidisciplinar, Universitat Politècnica de València, E-46022 Valencia, Spain.

<sup>2</sup>Institut de Matemàtiques i Aplicacions de Castelló and Departament de Matemàtiques, Universitat Jaume I, E-12071 Castellón, Spain.

<sup>3</sup>Konputazio Zientziak eta A.A. saila, Informatika Fakultatea, UPV/EHU, Donostia/San Sebastián, Spain.

## 1 Introduction

When investigating the dynamical behavior of quantum systems of low to moderate dimension, very often it is necessary to solve numerically the time dependent Schrödinger equation ( $\hbar = 1$ )

$$i\hbar \frac{\partial}{\partial t} \psi(x, t) = \hat{H} \psi(x, t), \quad \psi(x, 0) = \psi_0(x). \quad (1)$$

---

\*Email: serblaza@imm.upv.es

†Email: Fernando.Casas@uji.es

‡Email: Ander.Murua@ehu.es

Here  $\hat{H}$  is the Hamiltonian operator,  $\psi : \mathbb{R}^d \times \mathbb{R} \rightarrow \mathbb{C}$  is the wave function representing the state of the system and  $\psi_0(x)$  is the initial state. For simplicity, in the sequel we consider  $\hat{H} = \hat{T} + \hat{V}$ , with the kinetic energy operator  $\hat{T} = -\Delta/(2\mu)$  for a reduced mass  $\mu > 0$  and a potential  $\hat{V}$ , although the procedure presented in this paper is also valid for more general Hamiltonian operators.

The solution of (1) can be expressed as

$$\psi(x, t) = \hat{U}(t)\psi_0(x), \quad (2)$$

the (unitary) evolution operator  $\hat{U}$  being formally given by  $\hat{U}(t) = e^{-it\hat{H}}$ . In practice, however, it is not possible to get a closed expression for  $\hat{U}(t)$ , and so numerical methods are applied to get reliable approximations. This process involves typically two stages. In the first a discrete spatial representation of the initial wave function  $\psi_0(x)$  and the operator  $\hat{H}$  on an appropriate grid are constructed. In the second, this finite representation is propagated in time with a numerical integrator.

As for the space discretization process, several techniques can be used, depending on the particular problem one aims to analyze: finite difference schemes, spectral methods based on collocation with trigonometric polynomials, Galerkin method with a Hermite basis, etc, both in one or more dimensions (see [15] and references therein). The space discretization process restricts the energy range of the approximation and imposes an upper bound to the high frequency components represented by the discrete solution.

In any event, once this process has been carried out, one has the linear system of ordinary differential equations

$$i \frac{d}{dt} u(t) = H u(t), \quad u(0) = u_0 \in \mathbb{C}^N, \quad (3)$$

where  $u(t)$  now represents a discretized version of the wave function  $\psi(x, t)$  at the  $N$  space grid points, with  $N$  usually a large number. The goal is then to compute  $u(t)$  at a given target time  $t$  from the known value of  $u(0) = u_0$ . The  $N \times N$  matrix  $H$  (and in particular its discrete spectrum) depends of course on the particular space discretization carried out. We will hereafter assume that  $H$  is a real symmetric matrix which implies that it can be diagonalized with real eigenvalues.

The exact solution of eq. (3) reads

$$u(t) = e^{-itH} u_0, \quad (4)$$

but computing the matrix exponential  $e^{-itH}$  by diagonalizing  $H$  (usually, a matrix of large dimension and large norm) is prohibitively expensive. An effective alternative consists in computing approximations of  $u(t)$  of the form

$$u(t) \approx P_m(tH)u_0, \quad (5)$$

where  $P_m(y)$  is a polynomial in  $y$  that approximates the exponential  $e^{-iy}$ , since in that case only multiplications of the matrix  $H$  with vectors  $u$  are necessary. These products can be efficiently evaluated in complex variables (provided that

a Fourier spectral method is used to obtain the discretized version (3) of (1) with the complex-to-complex Fast Fourier Transform (FFT) algorithm [5, 11, 12, 13].

There are different choices for such a polynomial  $P_m(y)$ . For instance, one may consider truncated Taylor or Chebyshev series expansion of  $e^{-iy}$  for an appropriate real interval of  $y$ , or the Lanczos method, where the polynomial is determined by a Galerkin approximation on the Krylov space spanned by  $u_0, Hu_0, \dots, H^{m-1}u_0$  [18].

In this paper we consider yet another kind of polynomial approximation to  $e^{-itH}u_0$ , namely one based on explicit symplectic splitting methods [7, 8, 1, 2, 3]. This approach can be applied under the same assumptions than the Chebyshev method, the main difference being the following. Whereas in the Chebyshev (or Taylor) method the approximation (5) is constructed by evaluating products of the form  $Hu$ , where  $u \in \mathbb{C}^N$ , with symplectic splitting methods one writes  $u = q + ip$ ,  $q, p \in \mathbb{R}^N$ . The algorithm then proceeds by successively computing *real* matrix-vector products  $Hq$  and  $Hp$  with different weights, so that the real and imaginary parts of  $e^{-itH}u_0$  are approximated in a different way, with a much reduced computational cost.

More specifically, if a spatial discretization based on Fourier spectral methods is considered, then the cost of computing  $Hu$ ,  $u \in \mathbb{C}^N$ , amounts essentially to one complex-to-complex FFT and its inverse, whereas in the case of  $Hv$ ,  $v \in \mathbb{R}^N$ , one has to evaluate one real-to-complex FFT and its inverse complex-to-real FFT, and this process requires half the computing time of the fully complex case. As a result, the proposed algorithm based on splitting methods turns out to be between 1.4 and 2 times faster than the Chebyshev method for the same accuracy in all the examples we have analyzed. Moreover, the procedure is easy to implement and the resulting approximations preserve important qualitative properties of the exact solution.

The algorithm we present here has embedded several symplectic splitting schemes designed according to different optimization criteria with the purpose of covering most of the cases one finds in practical applications (high accuracy over long time intervals, low accuracy over short times, etc.). The computation of the coefficients of the methods, which constitutes a non-trivial task by itself, is largely based on the stability and error analysis of splitting methods carried out in [2, 3]. Given a target value of time  $t$  and an error tolerance, the algorithm selects a specific symplectic splitting scheme leading to a numerical solution with the prescribed accuracy and the minimum computational work, measured as the number of real matrix-vector products. By construction, the algorithm developed here is aimed to be applied for the same problems and under the same assumptions as the Chebyshev method, with a remarkable gain in efficiency for all the examples we have tested.

The plan of the paper is the following. Since our procedure may be considered as an alternative to the Chebyshev method, in section 2 we summarize the main features of the schemes based on this polynomial approximation of  $e^{-itH}u_0$ . In section 3 we analyze the stability and the global error of symplectic splitting methods in this context, and the actual algorithm is presented, whereas the comparison with Chebyshev (and Taylor as a reference) is carried

out in section 4 on a pair of selected numerical examples.

## 2 Polynomial approximations

### 2.1 General considerations

Given a  $m$ th degree polynomial  $P_m(y)$  approximating  $e^{-iy}$ , the solution  $u(t) = e^{-itH}u_0$  of (3) at a prescribed target time  $t$  can be approximated as

$$u(t) \approx u_1 = P_m(tH)u_0, \quad (6)$$

with the corresponding error (in Euclidean norm) bounded as

$$\|u_1 - e^{-itH}u_0\| \leq \max_{j=0,1,\dots,N-1} |P_m(tE_j) - e^{-itE_j}| \|u_0\|$$

in terms of the (real) eigenvalues  $E_0, \dots, E_{N-1}$  of  $H$ . Assuming that the spectrum  $\sigma(H) = \{E_0, \dots, E_{N-1}\}$  is contained in an interval of the form  $[E_{\min}, E_{\max}]$ , then

$$\|u_1 - e^{-itH}u_0\| \leq \sup_{tE_{\min} \leq y \leq tE_{\max}} |P_m(y) - e^{-iy}| \|u_0\|.$$

There are several possibilities to estimate  $E_{\max}$  and  $E_{\min}$  for different classes of matrices (see e.g. [9, 16, 21, 22]). If  $H$  can be decomposed as the sum  $H = T + V$  of two symmetric matrices with known lower and upper bounds for their eigenvalues,  $E_{\min}$  (resp.  $E_{\max}$ ) can be simply obtained as the sum of the lower (resp. upper) bounds of the eigenvalues of  $T$  and  $V$ . This happens, in particular, when the Hamiltonian operator  $\hat{H} = -\Delta/(2\mu) + \hat{V}$  is discretized by spectral Fourier collocation with  $N$  Fourier modes, in which case

$$E_{\min} = \min_x V(x), \quad E_{\max} = \frac{1}{2\mu} \frac{N^2}{4} + \max_x V(x). \quad (7)$$

In any event, once  $E_{\min}$  and  $E_{\max}$  have been determined, we introduce

$$\alpha = \frac{E_{\max} + E_{\min}}{2}, \quad \beta = \frac{E_{\max} - E_{\min}}{2}, \quad \bar{H} = H - \alpha I, \quad (8)$$

so that the spectrum of the shifted operator  $\bar{H}$  is contained in an interval centered at the origin,  $\sigma(\bar{H}) = \{E_0 - \alpha, \dots, E_{N-1} - \alpha\} \subset [-\beta, \beta]$ . We thus have

$$e^{-itH}u_0 = e^{-it\alpha} e^{-it\bar{H}}u_0. \quad (9)$$

Hence, we will hereafter assume without loss of generality that our problem consists in approximating  $e^{-itH}u_0$  for a real symmetric matrix  $H$  with  $\sigma(H) \subset [-\beta, \beta]$ . In that case,

$$\|u_1 - e^{-itH}u_0\| \leq \epsilon_m(\beta t) \|u_0\|, \quad (10)$$

where

$$\epsilon_m(\theta) \equiv \sup_{-\theta \leq y \leq \theta} |e^{-iy} - P_m(y)|. \quad (11)$$

## 2.2 Taylor polynomial approximation

The  $m$ th degree Taylor polynomial  $P_m^T(y)$  corresponding to  $e^{-iy}$  is of course

$$P_m^T(y) \equiv \sum_{k=0}^m \frac{(-i)^k}{k!} y^k, \quad (12)$$

and Horner's algorithm provides an efficient way to compute  $u_1 = P_m^T(tH)u_0$ , namely

$$\begin{aligned} & y_0 = u_0 \\ & \mathbf{do} \quad k = 1, m \\ & \quad y_k = u_0 - i \frac{t}{m+1-k} H y_{k-1} \\ & \mathbf{enddo} \\ & u_1 = y_m. \end{aligned} \quad (13)$$

The process requires storing three complex vectors (or equivalently, 6 real vectors).

An error estimate of the form (10) can be obtained with  $\epsilon_m(\theta)$  in (11) replaced by its upper bound

$$\epsilon_m^T(\theta) \equiv \frac{\theta^{m+1}}{(m+1)!}. \quad (14)$$

Since  $m! \sim \sqrt{2\pi m} (me)^m$  for large values of  $m$  [17], we can write

$$\epsilon_m^T(\theta) \sim \frac{1}{e\sqrt{2\pi m}} \left(\frac{\theta e}{m}\right)^{m+1}.$$

In consequence, we cannot expect to have a reasonably accurate approximation  $P_m^T(tH)u_0$  of  $e^{-itH}u_0$  unless

$$m > e\theta = e\beta t.$$

In other words, increasing the value of the target time  $t$  where the solution is to be found and/or refining the spatial discretization (so that  $\beta$  gets larger) requires evaluating a higher degree Taylor polynomial.

## 2.3 Chebyshev polynomial approximation

The Chebyshev polynomial expansion scheme, proposed for the first time in the context of the Schrödinger equation in [19], constitutes a standard tool to compute (4). A detailed analysis of the procedure, including error estimates for the problem at hand, can be found in [15]. For completeness, we review here some of its main features.

The  $m$ th degree truncation of the Chebyshev series expansion of  $e^{-iy}$  in the interval  $y \in [-\theta, \theta]$  is given by

$$P_{m,\theta}^C(y) \equiv J_0(\theta) + 2 \sum_{k=1}^m (-i)^k J_k(\theta) T_k(y/\theta), \quad (15)$$

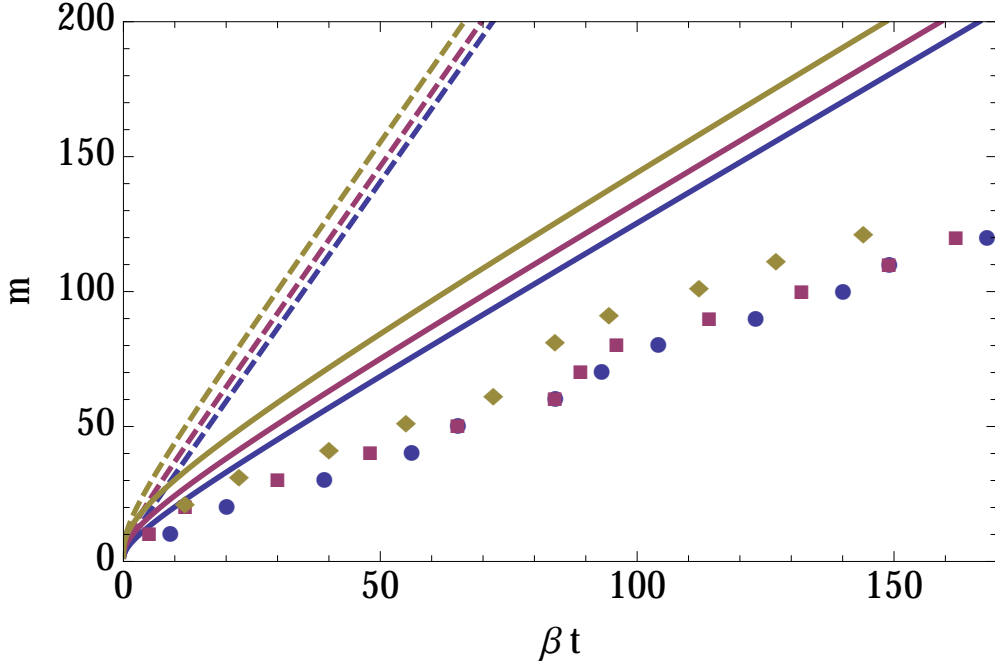


Figure 1: Comparison of the required minimum polynomial degree  $m$  as function of  $\theta = \beta t$  for Taylor (dashed line) and Chebyshev (continuous line) for different values of error tolerance:  $\text{tol} = 10^{-4}, 2 \times 10^{-7}, 10^{-11}$ . Diamonds, squares and circles stand for the computational cost (equivalent to a polynomial approximation of degree  $m$ ) for error tolerances below  $10^{-4}$ ,  $2 \times 10^{-7}$  and  $10^{-11}$ , respectively, obtained with symplectic splitting schemes in Table 1.

where for each  $k$ ,  $J_k(t)$  is the Bessel function of the first kind [17] and  $T_k(x)$  is the  $k$ th Chebyshev polynomial generated from the recursion

$$T_{k+1}(x) = 2xT_k(x) - T_{k-1}(x), \quad k \geq 1 \quad (16)$$

and  $T_0(x) = 1$ ,  $T_1(x) = x$ . According with the analysis in [15],  $e^{-itH}u_0$  can be approximated by  $P_{m,\beta t}^C(tH)u_0$  with an error estimate of the form (10), where  $\epsilon_m(\theta)$  in (11) is replaced by its upper bound

$$\epsilon_m^C(\theta) \equiv 4 \left( e^{1-\theta^2/(2m+2)^2} \frac{\theta}{2m+2} \right)^{m+1}. \quad (17)$$

In Figure 1 we depict the minimum degree  $m$  as a function of  $\theta = \beta t$  of Chebyshev approximations for prescribed tolerances  $\text{tol} = 10^{-4}, 2 \times 10^{-7}, 10^{-11}$ , so that  $\epsilon_m^C(\beta t) \leq \text{tol}$  (continuous lines) in comparison with the corresponding degree  $m$  for Taylor approximations (dashed lines) such that  $\epsilon_m^T(\beta t) \leq \text{tol}$ . Notice that Chebyshev always gives a similar accuracy with a lower degree polynomial (hence, with less computational cost), with a gain in efficiency of up to a factor of two for sufficiently large values of  $\theta = \beta t$ .

Once the degree of the polynomial  $m$  has been chosen, given a certain error tolerance, target time  $t$ , and bound  $\beta$  of  $\sigma(H)$ , one has to compute  $P_{m,\beta t}^C(tH)u_0$

in an as efficient as possible way. This can be done with the Clenshaw recursive algorithm as follows: first evaluate the coefficients  $c_k = (-1)^k J_k(\beta t)$  for  $k = 0, 1, \dots, m$  and then compute recursively

$$\begin{aligned}
& d_{m+2} = 0, \quad d_{m+1} = 0 \\
& \mathbf{do} \quad k = m, m-1, \dots, 1, 0 \\
& \quad d_k = c_k u_0 + \frac{2}{\beta} H d_{k+1} - d_{k+2} \\
& \mathbf{enddo} \\
& u_1 = d_0 - d_2,
\end{aligned} \tag{18}$$

which produces  $u_1 \equiv P_{m,\beta t}^C(tH) u_0 \approx e^{-itH} u_0$  as output. Clenshaw algorithm keeps only four complex vectors in memory<sup>1</sup>, but the whole procedure has to be carried out for each value of  $m$ . Since the coefficients  $c_k$  are relatively small as  $k$  grows, the Clenshaw algorithm is stable and so it is possible to work with polynomials of very high degree (even in the thousands) provided the Bessel functions are accurately computed.

### 3 Symplectic splitting methods

#### 3.1 General considerations

An alternative to Chebyshev polynomial approximations of  $e^{-itH} u_0$  first considered in [7, 8] consists in applying specially designed splitting methods to numerically integrate the system (3) recast in a more suitable form.

By considering  $q = \operatorname{Re}(u) \in \mathbb{R}^N$  and  $p = \operatorname{Im}(u) \in \mathbb{R}^N$ , equation (3) is equivalent to

$$\frac{d}{dt} z = (A + B)z, \quad z(0) = z_0, \tag{19}$$

where

$$z = \begin{pmatrix} q \\ p \end{pmatrix}, \quad A = \begin{pmatrix} 0 & H \\ 0 & 0 \end{pmatrix}, \quad B = \begin{pmatrix} 0 & 0 \\ -H & 0 \end{pmatrix}. \tag{20}$$

The solution  $z(t) = e^{t(A+B)} z_0$  of (19) can be written in terms of the orthogonal and symplectic matrix

$$O(y) = \begin{pmatrix} \cos(y) & \sin(y) \\ -\sin(y) & \cos(y) \end{pmatrix} \tag{21}$$

as  $z(t) = O(tH) z_0$ . To introduce general symplectic splitting methods in this setting, let us first show how the well known Strang splitting can be used to approximate  $e^{-itH} u_0$ . Let  $m$  be a sufficiently large positive integer, so that for  $\tau = t/m$ , we consider the approximation

$$e^{\tau(A+B)} \approx e^{\frac{\tau}{2}A} e^{\tau B} e^{\frac{\tau}{2}A}.$$

---

<sup>1</sup>If the vectors are written in their real and imaginary part, and the algorithm is carried out in real variables, then the algorithm needs to store only seven real vectors instead of eight.

It is then clear that

$$e^{t(A+B)} = \left( e^{\tau(A+B)} \right)^m \approx \left( e^{\frac{\tau}{2}A} e^{\tau B} e^{\frac{\tau}{2}A} \right)^m = e^{\frac{\tau}{2}A} \left( e^{\tau B} e^{\tau A} \right)^{m-1} e^{\tau B} e^{\frac{\tau}{2}A},$$

or equivalently,

$$O(tH) = e^{t(A+B)} \approx K(tH) = e^{ta_{m+1}A} e^{tb_m B} e^{ta_m A} \dots e^{tb_1 B} e^{ta_1 A}, \quad (22)$$

with

$$(a_1, b_1, a_2, \dots, a_m, b_m, a_{m+1}) = \left( \frac{1}{2m}, \frac{1}{m}, \frac{1}{m}, \dots, \frac{1}{m}, \frac{1}{m}, \frac{1}{2m} \right). \quad (23)$$

Due to the nilpotent structure of the matrices  $A$  and  $B$  in (20), the exponentials in the definition (22) of  $K(tH)$  take a particularly simple form, namely

$$e^{ta_j A} = \begin{pmatrix} I & a_j t H \\ 0 & I \end{pmatrix}, \quad e^{tb_j B} = \begin{pmatrix} I & 0 \\ -b_j t H & I \end{pmatrix}. \quad (24)$$

This analysis shows that the approximation  $K(tH)z_0 \approx e^{t(A+B)}z_0$  can be computed with the following procedure, similar in nature and equivalent in computing time to the Horner (13) and Clenshaw (18) algorithms: Given  $u_0 \in \mathbb{C}^N$ ,

$$\begin{aligned} q &:= \operatorname{Re}(u_0), \\ p &:= \operatorname{Im}(u_0), \\ \mathbf{do} \quad k &= 1, m \\ \quad q &:= q + a_k t H p \\ \quad p &:= p - b_k t H q \\ \mathbf{enddo} \\ q &:= q + a_{m+1} t H p \\ u_1 &:= q + ip, \end{aligned} \quad (25)$$

producing  $u_1 \approx e^{-itH}u_0$  as output. Notice that it only requires storing three real vectors of dimension  $N$  (namely  $q$ ,  $p$ , and  $w = Hp$  or  $w = Hq$ ) instead of seven real vectors for the Clenshaw algorithm and six real vectors for the Horner algorithm. It is worth remarking that, since  $e^A$  and  $e^B$  are symplectic matrices,  $K(tH)$  is also symplectic. Unitarity is no longer preserved by this scheme, but neither the average error in energy nor the norm of the solution increases with time, since it is conjugate to a unitary method [2].

In practice, and in the same way as other polynomial approximations, it is convenient to apply Algorithm (25) with the original  $H$  replaced by the shifted version  $\bar{H}$  considered in (8) (and then make use of the equality (9)), so that the spectrum of  $\bar{H}$  is contained in an interval of the form  $[-\beta, \beta]$  with  $\beta$  as sharp as possible. Therefore, in what follows we always assume that  $\sigma(H) \subset [-\beta, \beta]$ .

Although Algorithm (25) with coefficients (23) can be used in principle to approximate  $e^{-itH}u_0$ , we next show that, for given values of  $m$  and  $\theta = \beta t$ , much better approximations can be obtained if other sequences of coefficients  $(a_1, b_1, a_2, \dots, a_m, b_m, a_{m+1})$  are chosen instead. To see how this can be done, an error estimate of the corresponding approximation (22) is necessary first.



### 3.2 Error analysis

For a given finite sequence of real numbers

$$(a_1, b_1, a_2, \dots, a_m, b_m, a_{m+1}), \quad (26)$$

Algorithm (25) produces an approximation of the form

$$\begin{pmatrix} q_1 \\ p_1 \end{pmatrix} = K(tH) \begin{pmatrix} q_0 \\ p_0 \end{pmatrix} \approx e^{t(A+B)} \begin{pmatrix} q_0 \\ p_0 \end{pmatrix}$$

(or equivalently,  $q_1 + i p_1 \approx e^{-itH}(q_0 + i p_0)$ ) with

$$K(tH) = \begin{pmatrix} K_{11}(tH) & K_{12}(tH) \\ K_{21}(tH) & K_{22}(tH) \end{pmatrix}. \quad (27)$$

Here  $K_{11}(y)$ ,  $K_{22}(y)$  are even polynomials of degree  $2m$ ,  $K_{12}(y)$  and  $K_{21}(y)$  are odd polynomials of degree  $2m - 1$  and  $2m + 1$  respectively, and  $\det K(y) = K_{11}(y)K_{22}(y) - K_{12}(y)K_{21}(y) \equiv 1$ . It is important to remark that for a given positive integer  $m$ , compared to Horner's (13) and Clenshaw's (18) algorithms, the degree of the polynomials involved in an  $m$ -stage splitting method (26) is *twice* the degree of the corresponding Taylor and Chebyshev polynomials, with the same computational cost.

#### 3.2.1 Error estimates for a single application of a splitting method

We next focus on obtaining upper bounds for the error

$$\begin{aligned} \|(q_1 + i p_1) - e^{-itH}(q_0 + i p_0)\| &= \left\| K(tH) \begin{pmatrix} q_0 \\ p_0 \end{pmatrix} - O(tH) \begin{pmatrix} q_0 \\ p_0 \end{pmatrix} \right\| \\ &\leq \|K(tH) - O(tH)\| \|q_0 + i p_0\| \end{aligned}$$

in Euclidean norm. Since  $H$  is assumed to be a real symmetric matrix, it can be diagonalized as

$$H = P^T \begin{pmatrix} E_0 & 0 & \cdots & 0 \\ 0 & E_1 & \cdots & 0 \\ 0 & 0 & \ddots & 0 \\ 0 & \cdots & 0 & E_{N-1} \end{pmatrix} P,$$

where  $P$  is an orthogonal  $N \times N$  matrix. We thus have

$$K(tH) - O(tH) = P^T \mathcal{E} P,$$

where  $\mathcal{E}$  is the block-diagonal matrix (with  $2 \times 2$  matrices at the diagonal)

$$\begin{pmatrix} K(tE_0) - O(tE_0) & 0 & \cdots & 0 \\ 0 & K(tE_1) - O(tE_1) & \cdots & 0 \\ 0 & 0 & \ddots & 0 \\ 0 & \cdots & 0 & K(tE_{N-1}) - O(tE_{N-1}) \end{pmatrix},$$

and therefore

$$\|K(tH) - O(tH)\| \leq \|\mathcal{E}\| = \max_{j=0,1,\dots,N-1} \|K(tE_j) - O(tE_j)\|.$$

Since  $|E_j| \leq \beta$ ,  $j = 0, 1, \dots, N-1$ , we finally arrive at

$$\|(q_1 + ip_1) - e^{-itH}(q_0 + ip_0)\| \leq \epsilon(\beta t) \|q_0 + ip_0\|, \quad (28)$$

where

$$\epsilon(\theta) = \sup_{-\theta \leq y \leq \theta} \|K(y) - O(y)\|. \quad (29)$$

By taking into account that  $\det K(y) \equiv 1$ , the 2-norm of the  $2 \times 2$  matrix  $K(y) - O(y)$  can be explicitly computed to give

$$\|K(y) - O(y)\| = \sqrt{(C(y) - \cos(y))^2 + (S(y) - \sin(y))^2} + \sqrt{C(y)^2 + S(y)^2 - 1},$$

where

$$C(y) = \frac{1}{2}(K_{11}(y) + K_{22}(y)), \quad S(y) = \frac{1}{2}(K_{12}(y) - K_{21}(y)). \quad (30)$$

Notice that  $\det K(y) \equiv 1$  implies

$$C(y)^2 + S(y)^2 - 1 = \frac{1}{4}(K_{11}(y) - K_{22}(y))^2 + \frac{1}{4}(K_{12}(y) + K_{21}(y))^2$$

and thus  $C(y)^2 + S(y)^2 - 1 \geq 0$  for all real values of  $y$ .

### 3.2.2 Error estimates for several steps of a splitting method

Ideally, given a positive integer  $m$  and  $\theta = \beta t > 0$ , one would like to determine a sequence (26) of real numbers so that  $\epsilon(\theta)$  is minimized. The error bound  $\epsilon(\theta)$  being small implies that the  $(2m)$ th degree polynomial  $C(y)$  (resp. the  $(2m+1)$ th degree polynomial  $S(y)$ ) is a good polynomial approximation of  $\cos(y)$  (resp.  $\sin(y)$ ) for  $y \in [-\theta, \theta]$ , which implies that increasingly large values of  $\theta = \beta t$  will require longer sequences of coefficients (that is, larger values of  $m$ ), and consequently more computational work. The situation here is in complete analogy with what happened to Taylor and Chebyshev polynomial approximations in the previous section.

By applying the methodology exposed in [3] we have determined several sequences (26) of length  $2m+1$  of (near-to-optimal) coefficients for  $m$  up to 60. The procedure is described in detail in the Appendix. As shown there, the task is by no means trivial, and severe technical difficulties arise when trying to extend the procedure to arbitrarily large values of  $\theta = \beta t$  (and hence arbitrarily long sequences of coefficients). This is in contrast with Taylor and Chebyshev approximations.

This drawback can always be circumvented by approximating the solution  $z(t) = O(tH)z_0$  of the system of ordinary differential equations (19) in the standard step-by-step way. In our case, approximating  $z(t)$  in  $n$  steps of length

$$\tau = \frac{t}{n}$$

simply consists in approximating  $O(tH)z_0 = O(n\tau H)z_0 = O(\tau H)^n z_0$  by the vector  $K(\tau H)^n z_0$ , where  $K(y)$  is a  $2 \times 2$  matrix with polynomial entries (defined in terms of the sequence (26) as before) that should approximate the rotation matrix  $O(y)$  for  $y \in [-\frac{\beta t}{n}, \frac{\beta t}{n}]$ .

Clearly, the resulting procedure for approximating  $e^{-itH}u_0$  can be written as an algorithm of the form (25), corresponding to a sequence of coefficients (with a  $(2m)$ -periodic pattern) of length  $2nm + 1$ . The corresponding error can be estimated as

$$\begin{aligned} \|(q_1 + ip_1) - e^{-itH}(q_0 + ip_0)\| &\leq \|K(\tau H)^n - O(n\tau H)\| \|q_0 + ip_0\| \\ &\leq \epsilon^{(n)}(\tau\beta) \|q_0 + ip_0\|, \end{aligned} \quad (31)$$

where

$$\epsilon^{(n)}(\theta) = \sup_{-\theta \leq y \leq \theta} \|K(y)^n - O(ny)\|.$$

Our goal is then to minimize  $\epsilon^{(n)}(\theta)$ . A reasonable requirement is that  $K(y)^n$  be bounded for all  $n$ . This only happens in general for a certain range of values of  $y$ . One thus defines the stability threshold  $y_*$  as the largest non negative real number such that  $K(y)^n$  is bounded independently of  $n \geq 1$  for all  $y \in (-y_*, y_*)$  [2]. In particular, for the sequence (23) corresponding to the application of  $m$  steps of the Strang splitting, the stability threshold is  $y_* = 2m$ . As a matter of fact,  $2m$  is precisely the maximal stability threshold a sequence of coefficients (26) of length  $2m + 1$  can achieve [10].

From the analysis carried out in [3], it is possible to show that

$$\begin{aligned} \|K(y)^n - O(ny)\| &\leq 2 \sin(n(\arccos(C(y)) - y)/2) \\ &\quad + \sqrt{\frac{S(y)^2}{1 - C(y)^2} - 1} + \frac{1}{2} \left( \frac{S(y)^2}{1 - C(y)^2} - 1 \right), \end{aligned}$$

provided that  $y \in [-y_*, y_*]$ . This implies that, if  $\tau\beta \leq y_*$ , then

$$\begin{aligned} \|K(\tau H)^n - O(n\tau H)\| &\leq \sup_{-\tau\beta \leq y \leq \tau\beta} \|K(y)^n - O(ny)\| = \epsilon^{(n)}(\tau\beta) \\ &\leq n\mu(\tau\beta) + \nu(\tau\beta), \end{aligned} \quad (32)$$

where

$$\mu(\theta) = \sup_{-\theta \leq y \leq \theta} |\arccos(C(y)) - y|, \quad (33)$$

$$\nu(\theta) = \sup_{-\theta \leq y \leq \theta} \sqrt{\frac{S(y)^2}{1 - C(y)^2} - 1} + \frac{1}{2} \left( \frac{S(y)^2}{1 - C(y)^2} - 1 \right). \quad (34)$$

As mentioned before, we have determined several optimized splitting methods of  $m$  stages (determined by a sequence of coefficients (26) of length  $2m + 1$ ) for  $m$  up to 60. The relevant parameters of such splitting methods are collected in Table 1. In this table,  $M_m^{(\gamma)}$  refers to a method of  $m$  stages, with error coefficients  $\epsilon(\theta)$ ,  $\mu(\theta)$ ,  $\nu(\theta)$  optimized for  $\theta = \gamma m$ . For instance, method  $M_{60}^{(1,3)}$

can be used to approximate  $e^{-itH}u_0$  with an error bounded (according to (28) and Table 1) by  $1.2 \times 10^{-9}\|u_0\|$  provided that  $|t| \leq 78/\beta$ . Furthermore,  $e^{-itH}u_0$  can be approximated by applying  $n$  steps of length  $\tau = t/n \leq \tau_{\max} := 78/\beta$  of method  $M_{60}^{(1.3)}$  with an error bounded (according to (32)) by

$$(7.8n \times 10^{-11} + 1.2 \times 10^{-9})\|u_0\|.$$

In some cases two methods with the same values of  $m$  and  $\gamma = \theta/m$  have been collected, in which case they are labeled *a* and *b*. For instance, methods  $M_{60}^{(1.4)a}$  and  $M_{60}^{(1.4)b}$  are both designed to approximate  $e^{-itH}u_0$  with  $n$  steps of length  $\tau = t/n \leq \tau_{\max} := 84/\beta$  of the method. However, they differ in the actual error estimate (32): in the first case, the error is bounded (provided that  $\beta|t| \leq 84n$ ) by  $(2.4n \times 10^{-8} + 7.4 \times 10^{-8})\|u_0\|$ , while the second one admits the error estimate  $(3.7n \times 10^{-9} + 2.6 \times 10^{-6})\|u_0\|$ . This means that method  $M_{60}^{(1.4)a}$  will be more efficient if  $\beta|t| \leq 10452$ , and the opposite otherwise.

Thus, given the upper bound  $\beta$  of the spectral radius of  $H$  and the target time  $t$ , if one wants to approximate  $e^{-itH}u_0$  by applying  $n$  steps of method  $M_{60}^{(1.4)a}$ , one should choose the smallest positive integer  $n$  such that

$$\frac{t}{n} \leq \tau_{\max} := \frac{84}{\beta}, \quad \text{that is,} \quad n = \text{Ceiling}[t\beta/84].$$

For instance, suppose the target time  $t$  and the bound  $\beta$  are such that  $t\beta = 1000$ . Then, clearly,  $n = 12$ , so that 12 steps of scheme  $M_{60}^{(1.4)a}$  have to be applied with step size  $\tau = 1000/(12\beta) \simeq 83.3/\beta$  to achieve the target time. In this way one gets an approximation with estimated error of size  $3.62 \times 10^{-7}\|u_0\|$  with a computational work ( $2nm = 2 \times 12 \times 60 = 1440$  real matrix-vector products of the form  $Hv$ ) comparable to the use of a Chebyshev polynomial approximation of degree 720. In contrast, to guarantee a similar precision with Chebyshev, a polynomial of degree at least 1135 is required, since this is the minimum value of  $m$  such that  $\epsilon_m^C(1000)\|u_0\| \leq 3.62 \times 10^{-7}\|u_0\|$ , with  $\epsilon_m^C(\theta)$  given in (17).

It is worth remarking the error coefficients for Strang splitting method (23) with the same value of  $\gamma = \theta/m = 1.4$  (also collected in Table 1) are much larger than for methods  $M_{60}^{(1.4)a}$  and  $M_{60}^{(1.4)b}$ .

### 3.2.3 Error estimates for combined splitting methods

Sometimes it is just more efficient to apply a combination of two different methods instead of  $n$  steps of the same scheme. For instance, suppose that  $t\beta = 177$  and we have an error tolerance of  $\text{tol} = 10^{-7}$ . If we use  $M_{60}^{(1.4)a}$  then  $t\beta/84 \simeq 2.1$  so that, according with the previous considerations, method  $M_{60}^{(1.4)a}$  has to be used with  $n = 3$  steps of size  $\tau = 59/\beta$ , much smaller than the value  $\tau_{\max} = 84/\beta$  for which the scheme has been designed. This would result in an approximation fulfilling the required error tolerance obtained with 360 real matrix-vector products of the form  $Hv$ . A better strategy would be the following: apply two steps of scheme  $M_{60}^{(1.4)a}$  with step size  $\tau_{\max} = 84/\beta$  to approximate  $w = e^{-i2\tau_{\max}H}u_0$  and then approximating  $e^{-i(t-2\tau_{\max})H}w$  by using

some other method with less stages. More generally, we take  $n = \text{Floor}[t\beta/84]$  steps of length  $\tau_{\max} = 84/\beta$  to get  $w = e^{-in\tau_{\max}H}u_0$  and then we approximate  $e^{-i(t-n\tau_{\max})H}w$  with another method of Table 1 involving less stages.

To decide which method has to be used for this last step, we need an error estimate for the approximation obtained with such a combination of two methods. Assume that we apply  $n$  steps of length  $\hat{\tau}$  of a method characterized by a  $2 \times 2$  matrix  $\hat{K}(y)$  with polynomial entries, followed by a step of length  $\tau$  of a method characterized by the matrix  $K(y)$ , where  $t = n\hat{\tau} + \tau$ . From the preceding considerations, it is enough to estimate  $\|K(\tau H)\hat{K}(\hat{\tau} H)^n - O(tH)\|$ . This can be done in terms of the functions  $\hat{\mu}(\theta)$ ,  $\hat{\nu}(\theta)$  associated to  $\hat{K}(y)$  as defined in subsection 3.2.2, and the error function  $\epsilon(\theta)$  associated to  $K(\theta)$  as in subsection 3.2.1, together with the following function associated to  $K(y)$ :

$$\delta(\theta) = \sup_{-\theta \leq y \leq \theta} \|K(y)\| - 1. \quad (35)$$

Indeed, one obtains the following error estimate:

$$\begin{aligned} \|K(\tau H)\hat{K}(\hat{\tau} H)^n - O(tH)\| &\leq \|K(\tau H) - e^{-i\tau H}\| \|O(n\hat{\tau}H)\| \\ &\quad + \|K(\tau H)\| \|\hat{K}(\hat{\tau} H)^n - O(n\hat{\tau}H)\| \quad (36) \\ &\leq \epsilon(\tau\beta) + (1 + \delta(\tau\beta))(n\hat{\mu}(\hat{\tau}\beta) + \hat{\nu}(\hat{\tau}\beta)). \end{aligned}$$

Since, as it can be noticed in Table 1,  $\delta(\theta) \simeq \epsilon(\theta) \ll 1$ , then we can take simply

$$\|K(\tau H)\hat{K}(\hat{\tau} H)^n - O(tH)\| \lesssim \epsilon(\tau\beta) + n\hat{\mu}(\hat{\tau}\beta) + \hat{\nu}(\hat{\tau}\beta). \quad (37)$$

It is worth remarking that such an approximation will require  $2(n\hat{m} + m) + 1$  real matrix-vector products of the form  $Hv$ , and thus is equivalent in complexity to the application of a (Chebyshev or Taylor) polynomial approximation of degree  $n\hat{m} + m$ .

### 3.3 Flow of the algorithm

Once a set of symplectic splitting methods constructed for providing approximations under different conditions are available (methods collected in Table 1) we still have to design a strategy to select the most appropriate scheme and step-size to carry out the numerical integration in time with the desired accuracy and a as small as possible computational cost.

The user has to provide the values for  $E_{\min}$  and  $E_{\max}$ , a subprogram to compute the product  $Hv$  for a given real vector  $v$ , the final integration time  $t$  and the desired error tolerance `tol`. The procedure then implements the shifting (8), computes the value of  $\beta$  and determines the normalized Hamiltonian  $H$ .

Next, the algorithm determines the most efficient method (or composition of methods) among the list of available schemes which provides the desired result: it chooses the cheapest method with error bounds below such tolerance and, if several methods with the same computational cost (same value of  $m$ ) satisfy this condition, the algorithm chooses the scheme with the smallest error bound. This can be achieved if one starts the search from the methods with the smallest value of  $m$  and, for each value of  $m$ , proceeds by decreasing accuracy, i.e. by

$M_m^{(\theta/m)}$	$m$	$\theta = \beta\tau_{\max}$	$y_*/m$	$\epsilon(\theta)$	$\mu(\theta)$	$\nu(\theta)$	$\delta(\theta)$
$M_{10}^{(0.5)}$	10	5	0.63	$3.6 \times 10^{-8}$	$8.7 \times 10^{-11}$	$9.8 \times 10^{-8}$	$3.6 \times 10^{-8}$
$M_{10}^{(0.9)}$	10	9	0.94	$3.4 \times 10^{-5}$	$2.9 \times 10^{-5}$	$1.1 \times 10^{-5}$	$6.0 \times 10^{-6}$
$M_{20}^{(0.6)}$	20	12	0.79	$1.6 \times 10^{-13}$	$1.4 \times 10^{-13}$	$5.8 \times 10^{-14}$	$2.5 \times 10^{-14}$
$M_{20}^{(1)}$	20	20	1.1	$4.1 \times 10^{-7}$	$1.8 \times 10^{-8}$	$4.8 \times 10^{-7}$	$4.0 \times 10^{-7}$
$M_{30}^{(0.75)}$	30	22.5	0.84	$8.1 \times 10^{-15}$	$3.3 \times 10^{-16}$	$1.5 \times 10^{-14}$	$7.9 \times 10^{-15}$
$M_{30}^{(1)}$	30	30	1.0	$4.1 \times 10^{-10}$	$1.9 \times 10^{-10}$	$3.1 \times 10^{-10}$	$2.6 \times 10^{-10}$
$M_{30}^{(1.3)}$	30	39	1.36	$2.3 \times 10^{-5}$	$5.2 \times 10^{-6}$	$2.2 \times 10^{-5}$	$2.0 \times 10^{-5}$
$M_{40}^{(1)}$	40	40	1.1	$1.8 \times 10^{-12}$	$4.9 \times 10^{-14}$	$2.4 \times 10^{-12}$	$1.8 \times 10^{-12}$
$M_{40}^{(1.2)}$	40	48	1.26	$2.1 \times 10^{-8}$	$2.1 \times 10^{-8}$	$5.3 \times 10^{-10}$	$4.7 \times 10^{-10}$
$M_{40}^{(1.4)}$	40	56	1.48	$1.48 \times 10^{-5}$	$4.0 \times 10^{-6}$	$1.7 \times 10^{-5}$	$1.7 \times 10^{-5}$
$M_{50}^{(1)}$	50	50	1.07	$4.5 \times 10^{-15}$	$4.5 \times 10^{-15}$	$2.0 \times 10^{-17}$	$1.8 \times 10^{-17}$
$M_{50}^{(1.1)}$	50	55	1.13	$4.5 \times 10^{-13}$	$4.2 \times 10^{-13}$	$4.1 \times 10^{-14}$	$3.5 \times 10^{-14}$
$M_{50}^{(1.2)}$	50	60	1.26	$5.4 \times 10^{-11}$	$2.7 \times 10^{-11}$	$3.8 \times 10^{-11}$	$3.4 \times 10^{-11}$
$M_{50}^{(1.3)a}$	50	65	1.32	$1.2 \times 10^{-8}$	$1.2 \times 10^{-8}$	$8.3 \times 10^{-10}$	$7.6 \times 10^{-10}$
$M_{50}^{(1.3)b}$	50	65	1.32	$5.9 \times 10^{-7}$	$9.5 \times 10^{-11}$	$6.1 \times 10^{-7}$	$5.9 \times 10^{-7}$
$M_{60}^{(1.1)}$	60	66	1.15	$7.2 \times 10^{-15}$	$7.2 \times 10^{-15}$	$2.6 \times 10^{-17}$	$2.2 \times 10^{-17}$
$M_{60}^{(1.2)a}$	60	72	1.3	$1.5 \times 10^{-12}$	$1.1 \times 10^{-12}$	$8.3 \times 10^{-13}$	$7.5 \times 10^{-13}$
$M_{60}^{(1.2)b}$	60	72	1.26	$4.2 \times 10^{-11}$	$6.5 \times 10^{-14}$	$4.6 \times 10^{-11}$	$4.2 \times 10^{-11}$
$M_{60}^{(1.3)}$	60	78	1.36	$1.2 \times 10^{-9}$	$7.8 \times 10^{-11}$	$1.2 \times 10^{-9}$	$1.2 \times 10^{-9}$
$M_{60}^{(1.4)a}$	60	84	1.41	$8.4 \times 10^{-8}$	$2.4 \times 10^{-8}$	$7.4 \times 10^{-8}$	$7.1 \times 10^{-8}$
$M_{60}^{(1.4)b}$	60	84	1.46	$2.9 \times 10^{-6}$	$3.7 \times 10^{-9}$	$2.9 \times 10^{-6}$	$2.9 \times 10^{-6}$
Strang	1	1	2	$1.8 \times 10^{-1}$	$4.7 \times 10^{-2}$	$1.5 \times 10^{-1}$	$1.3 \times 10^{-1}$
Strang	1	1.4	2	$5.1 \times 10^{-1}$	$1.5 \times 10^{-1}$	$4.0 \times 10^{-1}$	$4.0 \times 10^{-1}$
Strang	1	1.9	2	1.34862	0.606472	2.4894	1.1746

Table 1: Relevant parameters of several symplectic splitting methods especially designed to integrate the semi-discretized Schrödinger equation using a time step  $\tau = t/n$  with a maximum value  $\tau_{\max}$ . Here  $y_*$  stands for the stability threshold and  $\epsilon(\theta)$ ,  $\mu(\theta)$ ,  $\nu(\theta)$ , and  $\delta(\theta)$  (for  $\theta = \beta\tau_{\max}$ ) are the coefficients (appearing in the error estimates obtained in Subsection 3.2) given in (29), (32), and (35) respectively.

increasing the value of  $\theta = \beta\tau_{\max}$ . For a given value of  $t\beta$  and `tol` the algorithm checks for each method if  $t\beta \leq \beta\tau_{\max}$  and, if this condition is satisfied, then it examines if  $\epsilon(\theta) < \text{tol}$ . This procedure corresponds to the sequence of methods collected in Table 1 from top to bottom.

If none of the methods from the table satisfy both conditions for  $t\beta$  and `tol`, then the time integration is split, i.e.  $t\beta$  is divided and a composition of one or several methods is used instead. Due to the high performance of the methods with the largest number of stages (in this case 60) the algorithm examines the cost of  $n$  steps for the six 60-stage methods where  $n = \text{Floor}[t\beta/\tau_{\max}\beta]$  and the last step is carried using one method from the list of methods. It chooses the cheapest methods with the smaller error bound among the composition of methods which provide the desired accuracy.

In this way, if we denote by  $K_m^{(\gamma)}$  the matrix associated to method  $M_m^{(\gamma)}$ , then the resulting splitting method corresponds to the composition

$$K_m^{(\gamma_2)}(\tau\beta) \left( \hat{K}_{60}^{(\gamma_1)}(\hat{\tau}\beta) \right)^{n_1}, \quad (38)$$

where the algorithm chooses the methods (labelled by  $\gamma_1, \gamma_2, m$ ), the time steps,  $\tau, \hat{\tau}$ , and the value of  $n_1$ , where  $n_1 = 0$  if the method uses just one step. If  $n_1 > 0$  the error bound is given by (37) while for  $n_1 = 0$  the error bound is just  $\epsilon(\tau\beta)$ .

This strategy has been implemented as a Fortran code which is freely available for download at the website [20], together with some notes and examples illustrating the whole procedure.

In order to compare the efficiency of the resulting algorithm with the polynomial approximations based in Taylor and Chebyshev, with the error estimates collected in Table 1 we have represented in Figure 1 the computational work (equivalent to a polynomial approximation of degree  $m$ ) required for different tolerances and values of  $\beta t$ . Diamonds, squares and circles correspond to the error tolerances  $10^{-4}$ ,  $2 \cdot 10^{-7}$  and  $10^{-11}$ , respectively, obtained with one or several steps of schemes in Table 1. Notice that our algorithm based on symplectic splitting methods provide better accuracy with a considerably reduced computational effort.

## 4 Numerical examples

Next we apply the algorithm based on symplectic splitting methods presented in section 3 to two different examples and compare its main features with Chebyshev and Taylor polynomial approximations. For the first example, previously considered in [15] to illustrate Chebyshev and Lanczos approximations, we provide in addition the codes we have produced to generate the results and figures collected here. These can be found at [20]. The second example illustrates the performance of the methods on a one-dimensional Schrödinger equation with a smooth potential.

**Example 1.** The problem consists in computing  $u(t) = \exp(-it\tilde{H})u_0$  with  $u_0 \in \mathbb{C}^N$  a unitary random vector and the tridiagonal matrix

$$\tilde{H} = \frac{1}{2} \begin{pmatrix} 2 & -1 & & & \\ -1 & 2 & -1 & & \\ & & \ddots & & \\ & & & -1 & 2 & -1 \\ & & & & -1 & 2 \end{pmatrix} \in \mathbb{R}^{N \times N}. \quad (39)$$

The eigenvalues of  $\tilde{H}$  verify  $0 \leq E_k \leq 2$  for all  $k$ , so that we can take  $E_{\min} = 0$ ,  $E_{\max} = 2$ , and thus  $\alpha = \beta = 1$  in (8). In consequence, the problem reduces to approximate

$$e^{-iat} e^{-i\beta t H} u_0, \quad \text{where} \quad H = \tilde{H} - I. \quad (40)$$

We take  $N = 10000$  for the numerical experiments, but the results are largely independent of  $N$  (this is so even for the simplest, scalar case  $N = 1$ ).

Both Chebyshev and Taylor methods have been implemented in such a way that only real valued matrix-vector products are used (we always separate into the real and imaginary parts, i.e.  $Hu = H(q + ip) = Hq + iHp$ ), so that Chebyshev requires to store only 7 real vectors instead of 4 complex vectors.

We take as final time  $t = 20$  and measure the error in energy, the error in the preservation of unitarity and the tolerance for different values of  $m$ , the degree of the corresponding polynomials. The results are shown in Figure 2 with the following notation: dashed lines for the relative error in energy, solid lines for the error in unitarity, and dotted lines for the theoretical error bounds of the approximate solutions.

From the figure it is clear that the theoretical error bounds for the Taylor method are quite accurate for this example (since the bounds for  $E_{\min}$  and  $E_{\max}$  are sharp) and that for the effective time-step  $\tau\beta$  considered, the error is exceedingly large for  $m$  below reaching the super linear convergence regime. This is not the case for the Chebyshev method (notice that the estimate (17) is valid only for  $m > \tau\beta$ ) since the coefficients  $c_k$  of the polynomial (18) do not grow as much as in Taylor. We also depict the results achieved by the first two splitting methods with  $\tau_{\max}\beta \geq t\beta = 20$ ,  $M_{20}^{(1)}$  and  $M_{30}^{(0.75)}$ . For these schemes the corresponding relative error in energy is represented by filled squares, the error in unitarity by filled circles and the error bounds by crosses.

The relative performance of different numerical integrators is usually tested by measuring the error of the methods versus their computational cost. However, the splitting methods we are considering in this work are designed to achieve a given tolerance, whereas their computational cost is determined through the error bound estimate. For this reason, we believe it is more appropriate to measure the cost of the methods for different values of the tolerance. In particular, we take  $\text{tol} = 10^{-k}$ ,  $k = 1, 2, \dots, 12$  and final integration times  $t = 20, 50, 100, 200, 500, 1000$ . Figure 3 shows the results obtained with Chebyshev (line with squares) and the algorithm based on splitting schemes (line with circles) as a function of  $m$ . Even when high accuracy is required over long integration times (the most advantageous situation for Chebyshev approximations),



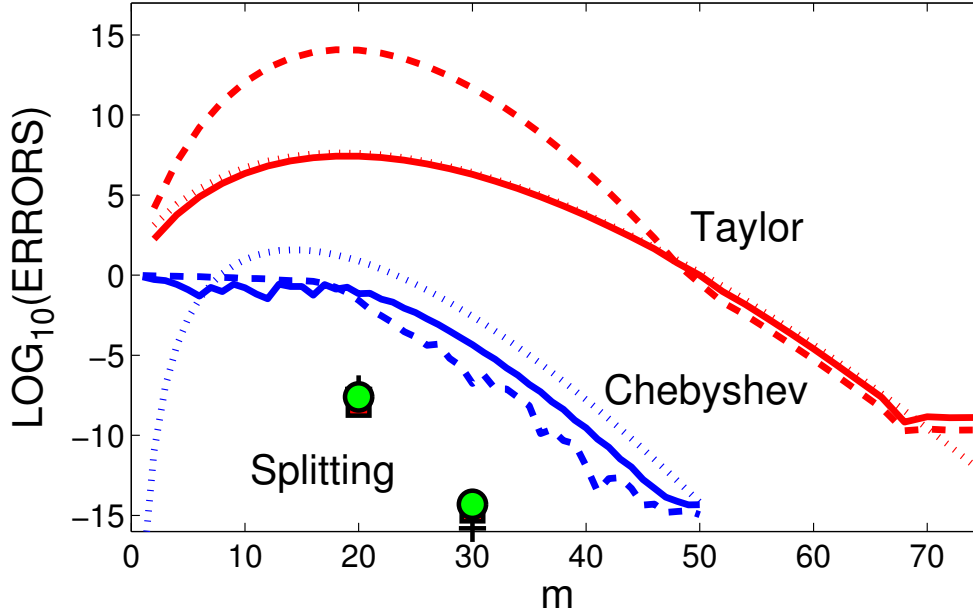


Figure 2: Different approximations to  $e^{-it\beta H}u_0$ , with  $H$  given in (39)-(40),  $u_0$  a random vector,  $\beta = 1$  and  $t\beta = 20$  versus the degree of the polynomials,  $m$ . The figure shows the relative error in energy (dashed lines), the error in unitarity (solid lines) and error bounds (dotted lines) for Chebyshev and Taylor methods. The results for the first two splitting methods with  $\beta\tau_{\max} \geq \beta t = 20$ ,  $M_{20}^{(1)}$  and  $M_{30}^{(0.75)}$ , are also shown: relative error in energy (filled squares), error in unitarity (filled squares) and error bounds (crosses).

the new algorithm requires a smaller value of  $m$  and therefore less computational effort. Notice how the algorithm selects the value of  $m$  to achieve the desired tolerance.

Figure 4 shows the corresponding results for the relative error in energy versus  $m$  for the same example. Similar results are obtained for the error in unitarity or the two-norm error for which the error bounds apply (in this case one should compute numerically the exact solution and compare with the approximations obtained for each value of `tol`).

**Example 2 (Pöschl–Teller potential).** To illustrate how the methods work on a more realistic case, we consider the well known one-dimensional Pöschl–Teller potential, which is an anharmonic quantum potential

$$V(x) = -\frac{a^2}{2\mu} \frac{\lambda(\lambda-1)}{\cosh^2(ax)},$$

with  $a > 0, \lambda > 1$ . It has been frequently used in polyatomic molecular simulation and is also of interest in supersymmetry, group symmetry, the study of solitons, etc. [4, 6, 14]. The parameter  $\lambda$  gives the depth of the well, whereas  $a$

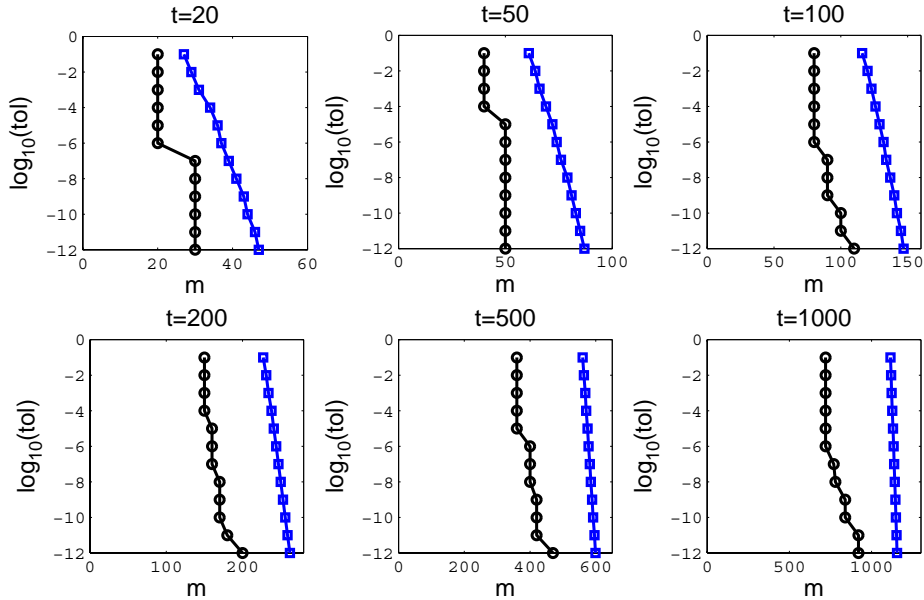


Figure 3: Degree  $m$  of the polynomials to achieve tolerances  $\text{tol} = 10^{-k}$ ,  $k = 1, 2, \dots, 12$  for different values of  $\beta t$  ( $\beta = 1$  for this problem) as determined by the error bound formulas using the Chebyshev method (squares) and the algorithm based on splitting methods (circles).

is related to the range of the potential. The energies are

$$E_k = -\frac{a^2}{2\mu}(\lambda - 1 - k)^2, \quad \text{with } 0 \leq k \leq \lambda - 1.$$

We take the following values for the parameters (in atomic units, a.u.): reduced mass  $\mu = 1745$  a.u.,  $a = 2$ ,  $\lambda = 24.5$  (leading to 24 bounded states), and  $x \in [-5, 5]$ . Moreover, to apply a pseudo spectral space discretization we assume periodicity of the potential in this range. The resulting  $V(x)$  is thus continuous and very close to differentiable for all  $x \in \mathbb{R}$ . Table 2 collects the bounds to the spectral radius (obtained according to (7)) and the corresponding shifting for the Pöschl–Teller potential when the space interval  $x \in [-5, 5]$  is split into  $N$  parts and for different values of  $N$ . Notice how sensibly  $E_{\max}$  depends on the space discretization.

We take as initial condition a Gaussian function,  $\psi(x, 0) = \sigma e^{-(3x)^2}$ , where  $\sigma$  is a normalizing constant, so the function and all its derivatives of practical interest vanish up to round off accuracy at the boundaries. The initial conditions contain part of the continuous spectrum, but this fact is largely irrelevant due to the smoothness of the periodic potential and wave function.

Suppose that one is interested in solving the corresponding semi discretized problem in time with the following requirements:

- (I)  $N = 128$ ,  $t = 15\pi$ ,  $\text{tol} = 10^{-9}$ . In this case  $t\beta = 26.4648$ .
- (II)  $N = 512$ ,  $t = 40\pi$ ,  $\text{tol} = 10^{-6}$ . Now  $t\beta = 507.254$ .

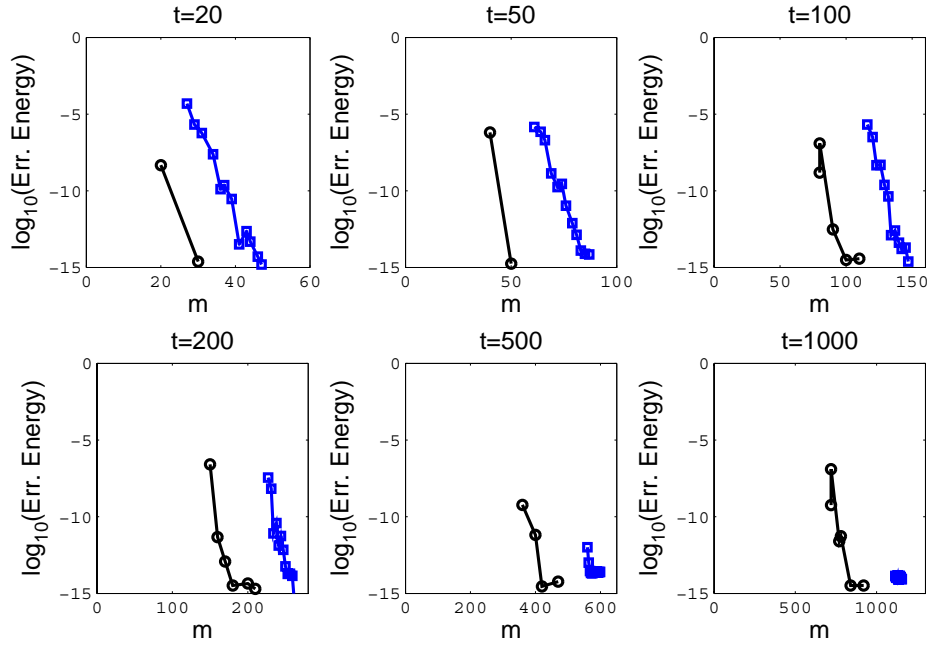


Figure 4: Same as Figure 3 but replacing the value of the tolerance `tol` by the relative error in energy.

We have to determine first, of course, the degree  $m$  of the polynomial from the corresponding error bounds (for Taylor the time interval is divided by two in (I) and by 36 in (II) to avoid exceedingly large round off errors). Table 3 shows the number of matrix-vector products used by each method (in bold) and the 2-norm error for each method (compared with the exact solution obtained numerically with very high accuracy). In the first case our algorithm makes the computations in a single step using  $M_{30}^{(1)}$  while in the second case it uses 6 steps of the scheme  $M_{60}^{(1.4)a}$  followed by one step of  $M_{10}^{(0.5)}$ , i.e. the composition (38) is now

$$K_{10}^{(0.5)}(\tau\beta) \left( \hat{K}_{60}^{(1.4)a}(\hat{\tau}\beta) \right)^6$$

with  $\hat{\tau} = 84/\beta$  and  $\tau = 40\pi - 6\hat{\tau}$ , and for a total of 370 products. Again, the algorithm based on symplectic splitting methods is able to produce results with the required accuracy with less computational effort.

## Acknowledgements

The authors acknowledge Ministerio de Economía y Competitividad (Spain) for financial support through the coordinated project MTM2013-46553-C3. AM is additionally partially supported by the Basque Government (Consolidated Research Group IT649-13), and FC by NPRP GRANT #5-674-1-114 from the Qatar National Research Fund.

$N$	$E_{\min}$	$E_{\max}$	$\alpha$	$\beta$
64	-0.65988	0.11583	-0.27202	0.38785
128	-0.65988	0.46333	-0.098275	0.5616
256	-0.65988	1.8533	0.59672	1.2566
512	-0.65988	7.4133	3.3767	4.0366
1024	-0.65988	29.653	14.496	15.156

Table 2: Bounds to the spectral radius and shifting for the Pöschl–Teller potential with the parameters considered in the text, when the space interval  $x \in [-5, 5]$  is split into  $N$  parts.

	<i>Taylor</i>	<i>Chebyshev</i>	<i>Symplectic</i>
$t\beta = 26.4648$ $\text{tol} = 10^{-9}$	<b>104</b> $3.4 \times 10^{-12}$	<b>51</b> $3.7 \times 10^{-12}$	<b>30</b> $4.2 \times 10^{-11}$
$t\beta = 507.254$ $\text{tol} = 10^{-6}$	<b>1836</b> $2.5 \times 10^{-8}$	<b>587</b> $3.4 \times 10^{-15}$	<b>370</b> $4.4 \times 10^{-9}$

Table 3: Number of matrix-vector products (in bold) and actual errors given by the Taylor, Chebyshev and symplectic methods for different  $t\beta$  and tolerances  $\text{tol}$ .

## References

- [1] S. Blanes, F. Casas, and A. Murua. Symplectic splitting operator methods tailored for the time-dependent Schrödinger equation. *J. Chem. Phys.*, 124:234105, 2006.
- [2] S. Blanes, F. Casas, and A. Murua. On the linear stability of splitting methods. *Found. Comp. Math.*, 8:357–393, 2008.
- [3] S. Blanes, F. Casas, and A. Murua. Error analysis of splitting methods for the time dependent Schrödinger equation. *SIAM J. Sci. Comput.*, 33:1525–1548, 2011.
- [4] S.-H. Dong. *Factorization Method in Quantum Mechanics*. Springer, 2007.
- [5] M.D. Feit, J.A. Fleck Jr., and A. Steiger. Solution of the Schrödinger equation by a spectral method. *J. Comp. Phys.*, 47:412–433, 1982.
- [6] S. Flügge. *Practical Quantum Mechanics*. Springer, 1971.
- [7] S. Gray and D.E. Manolopoulos. Symplectic integrators tailored to the time-dependent Schrödinger equation. *J. Chem. Phys.*, 104:7099–7112, 1996.
- [8] S. Gray and J.M. Verosky. Classical Hamiltonian structures in wave packet dynamics. *J. Chem. Phys.*, 100:5011–5022, 1994.

- [9] T.Z. Huang and R.S. Rau. A simple estimation for the spectral radius of (block) H-matrices. *J. Comput. Appl. Math.*, 177:455–459, 2005.
- [10] R. Jeltsch and O. Nevanlinna. Stability of explicit time discretizations for solving initial value problems. *Numer. Math.*, 37:61–91, 1981.
- [11] D. Kosloff and R. Kosloff. A Fourier method solution for the time dependent Schrödinger equation as a tool in molecular dynamics. *J. Comp. Phys.*, 52:35–53, 1983.
- [12] R. Kosloff. Time-dependent quantum mechanical methods for molecular dynamics. *J. Phys. Chem.*, 92:2087–2100, 1988.
- [13] C. Leforestier, R.H. Bisseling, C. Cerjan, M.D. Feit, R. Friesner, A. Guldberg, A. Hammerich, G. Jolicard, W. Karrlein, H.-D. Meyer, N. Lipkin, O. Roncero, and R. Kosloff. A comparison of different propagation schemes for the time dependent Schrödinger equation. *J. Comp. Phys.*, 94:59–80, 1991.
- [14] R. Lemus and R. Bernal. Connection of the vibron model with the modified Pöschl–Teller potential in configuration. *Chem. Phys.*, 283:401–417, 2002.
- [15] C. Lubich. *From Quantum to Classical Molecular Dynamics: Reduced Models and Numerical Analysis*. European Mathematical Society, 2008.
- [16] G. Mazzi and B.J. Leimkuhler. Dimensional reductions for the computation of time-dependent quantum expectations. *SIAM J. Sci. Comput.*, 33:2024–2038, 2011.
- [17] F.W.J. Olver, D.W. Lozier, R.F. Boisvert, and C.W. Clark. *NIST Handbook of Mathematical Functions*. Cambridge University Press, 2010.
- [18] T.J. Park and J.C. Light. Unitary quantum time evolution by iterative Lanczos reduction. *J. Chem. Phys.*, 85:5870–5876, 1986.
- [19] H. Tal-Ezer and R. Kosloff. An accurate and efficient scheme for propagating the time dependent Schrödinger equation. *J. Chem. Phys.*, 81:3967–3971, 1984.
- [20] <http://www.gicas.uji.es/software.html>. An efficient algorithm for the time integration of the Schrödinger equation.
- [21] M. Yang. A simple method for estimating the bounds of spectral radius of nonnegative irreducible matrices. *Appl. Math. E-Notes*, 11:67–72, 2011.
- [22] Q. Zhu, G.D. Hu, and L. Zeng. Estimating the spectral radius of a real matrix by discrete Lyapunov equation. *J. Diff. Equat. Appl.*, 17:603–611, 2011.

## Appendix: Construction of methods

We next describe the algorithm used to determine the coefficients (26) of length  $2m + 1$  for given  $m$  and  $\theta \in (0, 2m)$ .

Since all the error estimates in Subsection 3.2 depend exclusively on the even polynomial (of degree  $2m$ )  $C(y)$  and the odd polynomial (of degree  $2m + 1$ )  $S(y)$  given in (30), we first try to determine an appropriate pair of such polynomials satisfying the necessary conditions  $C(0) = 1$  and  $C(x)^2 + S(x)^2 - 1 > 0$  (for all  $x \in \mathbb{R}$ ). Such pair of polynomials is uniquely determined by a polynomial  $P(y) = C(y) + S(y)$  of degree  $2m + 1$  satisfying

$$P(0) = 1, \quad \frac{1}{2}(P(y)^2 + P(-y)^2) - 1 \geq 0. \quad (41)$$

Once an appropriate polynomial  $P(y) = C(y) + S(y)$  satisfying (41) is chosen, there is only a finite number of corresponding sequences (26), which can be effectively determined [2]. Since all of them share the same error estimates, we choose among them a sequence that minimizes

$$\sum_{j=1}^{m+1} |a_j| + \sum_{j=1}^m |b_j|.$$

We next focus on the effective construction of the polynomial  $P(y) = C(y) + S(y)$  of degree  $2m + 1$ .

On the one hand, in order that the expression  $\sqrt{C(y)^2 + S(y)^2 - 1}$  featuring in the error estimate (29) be small in the interval  $y \in [-\theta, \theta]$ ,

$$\sup_{-\theta \leq y \leq \theta} |\cos(y + e(y)) + \sin(y + e(y)) - P(y)| \quad (42)$$

should be small for some real valued function  $e(y)$ . On the other hand, minimizing

$$\sqrt{(C(y) - \cos(y))^2 + (S(y) - \sin(y))^2}$$

in the interval  $y \in [-\theta, \theta]$  is, provided that (42) is small enough, essentially equivalent to minimizing

$$\sup_{-\theta \leq y \leq \theta} |e(y)|. \quad (43)$$

To reduce the complexity of the final algorithm for determining the polynomial  $P(y)$ , we will try to minimize instead an alternative norm of  $e(y)$  that we introduce next. First observe that if

$$e(y) = \hat{e}_0 + \sum_{j \geq 1} \hat{e}_j T_j(y/\theta) \quad (44)$$

is the Chebyshev series expansion of the function  $e(y)$ , then

$$\sup_{-\theta \leq y \leq \theta} |e(y)| \leq \sum_{j \geq 0} |\hat{e}_j|. \quad (45)$$

This suggests that the right hand side of (45) may be a good alternative to the supremum norm for sufficiently smooth functions  $e(y)$ . For practical considerations, we will minimize instead the following alternative norm of the function  $e(y)$

$$\|e\|_\theta \equiv \sqrt{\sum_{j \geq 0} (\hat{e}_j)^2}. \quad (46)$$

Now, to determine the polynomial  $P(y) = C(y) + S(y)$  of degree  $2m + 1$ , we consider, for a given odd integer  $l$  such that  $m + 1 \leq l \leq 2m$ , a given set of nodes  $y_1, \dots, y_l$  symmetrically placed in the interval  $[-\theta, \theta]$ , and a given odd polynomial  $e(y)$  of degree  $l - 2$ , the polynomial  $P(y)$  of degree  $2l - 1$  interpolating in the Hermite sense the function  $\cos(y + e(y)) + \sin(y + e(y))$  for the nodes  $y_1, \dots, y_l$ . In particular, this implies that  $P(0) = 1$  and

$$C(y)^2 + S(y)^2 - 1 = \frac{1}{2}(P(y)^2 + P(-y)^2) - 1 = V(y)W(y)^2 \quad (47)$$

where  $W(y) = (y - y_1) \cdots (y - y_l)$ , and  $V(y)$  is an even polynomial of degree  $4m - 2l + 2$ . Thus,  $P(y)$  satisfies the necessary condition (41) if and only if  $V(y) \geq 0$  for all  $y$ .

Notice that the interpolation error (42) admits an upper bound of the form

$$\sup_{-\theta \leq y \leq \theta} |\cos(y + e(y)) + \sin(y + e(y)) - P(y)| \leq \frac{\eta}{(2l)!} \sup_{-\theta \leq y \leq \theta} W(y)^2, \quad (48)$$

where  $\eta > 0$  is an upper bound of the (absolute value of) the  $(2l)$ th derivative of the function  $\cos(y + e(y)) + \sin(y + e(y))$  in the interval  $y \in [-\theta, \theta]$ .

For a prescribed set of nodes  $y_1, \dots, y_l$ , we restrict the choice of the odd polynomial  $e(y)$  (of degree  $l - 2$ ) so that the Hermite interpolating polynomial  $P(y)$  is of degree  $2m + 1$  (which introduces  $2(l - m) - 2$  non-linear constraints on the non-zero coefficients  $\hat{e}_1, \hat{e}_3, \dots, \hat{e}_l$  of the polynomial  $e(y)$  given by (44)), and determine  $e(y)$  by minimizing the norm  $\|e\|_\theta$  for that restricted set of odd polynomials  $e(y)$  of degree  $l - 2$ . This produces a polynomial  $P(y)$  for each choice of the set of nodes  $y_1, \dots, y_l$ . It then remains to choose, for a prescribed positive odd integer  $l$ , such a set of nodes  $y_1, \dots, y_l$ .

The error estimate (48) suggests that a good choice for the interpolating nodes  $\{y_1, \dots, y_l\}$  may be given by the zeros of the Chebyshev polynomial  $T_l(y/\theta)$  of degree  $l$ , which corresponds to minimizing the supremum norm (in the interval  $[-\theta, \theta]$ ) of the polynomial  $W(y)$ . Notice that minimizing the alternative norm  $\|W\|_\theta$  also gives rise to the same set of nodes. It then only remains, for given odd positive number  $2m + 1$  and for given  $\theta > 0$ , to determine the number  $l$  of interpolating nodes, that should satisfy  $m + 1 \leq l \leq 2m$ . If  $l$  is too close to  $2m$ , then, very few degrees of freedom are left to minimize  $\|e\|_\theta$ , and if  $l$  is too close to  $m + 1$ , then the Hermite interpolating error (42) is too large, causing the norm of the function  $C(y)^2 + S(y)^2 - 1$  not being small enough, in addition to  $V(y)$  in (47) typically not being positive. We thus proceed by determining  $P(y) = C(y) + S(y)$  for different values of  $l$  close to  $(3m + 3)/2$ , and choosing, among those satisfying  $V(y) \geq 0$ , one having the best error coefficient  $\epsilon(\theta)$  defined in (29).

Unfortunately, choosing the interpolating nodes  $\{y_1, \dots, y_l\}$  as the zeros of the Chebyshev polynomial  $T_l(y/\theta)$  of degree  $l$  typically results in a polynomial  $P(y) = C(y) + S(y)$  that does not satisfy the stability condition

$$|C(y)| \leq 1, \quad y \in [-\theta, \theta], \quad (49)$$

so that the error coefficients  $\mu(\theta), \nu(\theta)$  are not well defined, and thus the resulting splitting method cannot be reliably used in a step-by-step manner for large values of  $t\beta$ . In order to produce splitting methods satisfying that stability condition for given  $\theta$ , we proceed iteratively to choose the interpolating nodes  $\{y_1, \dots, y_l\}$  and the corresponding polynomial  $P(y)$  as follows: As a first approximation, we require the set of nodes  $\{y_1, \dots, y_l\}$  to contain the set  $\{j\pi : j \in \mathbb{Z}, |j\pi| \leq \theta\}$  and determine the remaining nodes by minimizing the norm  $\|W\|_\theta$  of  $W(y) = (y - y_1) \cdots (y - y_l)$ . Once the polynomial  $P(y) = C(y) + S(y)$  is determined for that set of nodes  $\{y_1, \dots, y_l\}$ , we compute the set of zeros of  $C'(y) = 0$  that are included in the interval  $[-\theta, \theta]$  (that are typically close to  $\{j\pi : j \in \mathbb{Z}, |j\pi| \leq \theta\}$ ), and determine the remaining nodes by minimizing the norm  $\|W\|_\theta$  of  $W(y) = (y - y_1) \cdots (y - y_l)$ . Successive iteration of this process gives a sequence of polynomials  $P(y) = C(y) + S(y)$  that converge to a polynomial satisfying the stability condition (49).

As an example, we have obtained the method  $M_{60}^{(1.4)a}$  in Table 1 by following this procedure for  $m = 60$ ,  $\theta = 84$ , and  $l = 97$ , which has produced a splitting methods with sequence of coefficients (26) plotted in Figure 5.

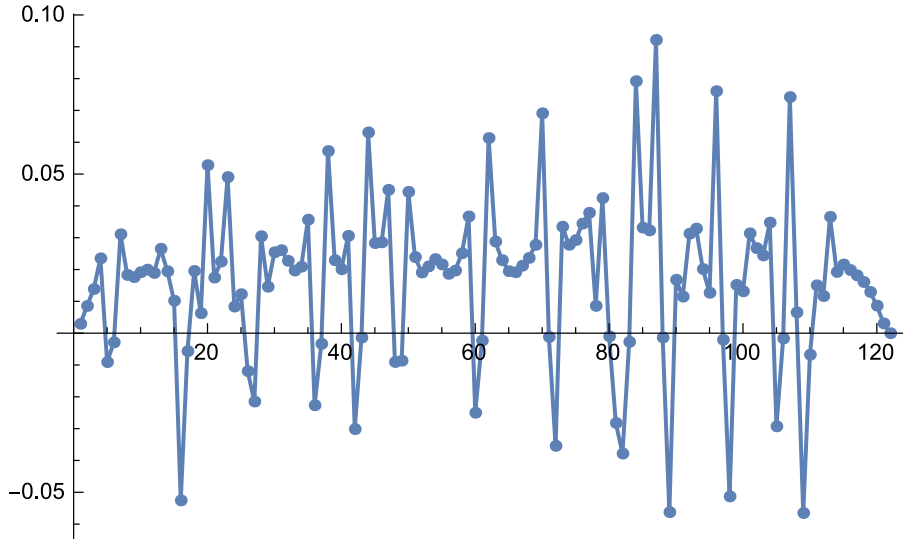


Figure 5: Graphical representation of sequence  $(a_1, b_1, a_2, b_2, \dots, a_{60}, b_{60}, a_{61})$  of method  $M_{60}^{(1.4)a}$  in Table 1, obtained with  $\theta = 84$  and  $l = 97$ .